Hindawi
Advances in Tribology
Volume 2018, Article ID 7575216, 7 pages
https://doi.org/10.1155/2018/7575216

Research Article

Experimental and Theoretical Analysis of Zircaloy-4 and AISI 304 Stainless Steel Material Pair in Water Sliding Conditions

Neelima Khare ,[1] Praveen Kumar Limaye,[1] Kulwant Singh,[2] Dhananjay Tatyasaheb Jadhav,[1] Arundhati Bute,[3] and Navnath Kalel[4]

[1]*Refueling Technology Division, Bhabha Atomic Research Centre, Mumbai 400085, India*
[2]*Materials Science Division, Bhabha Atomic Research Centre, Mumbai 400085, India*
[3]*Laser & Plasma Technology Division, Bhabha Atomic Research Centre, Mumbai 400085, India*
[4]*Department of Mechanical Engineering, Rajarambapu Institute of Technology, Sangli 415414, India*

Correspondence should be addressed to Neelima Khare; neelima.khare@gmail.com

Received 11 January 2018; Revised 16 April 2018; Accepted 29 May 2018; Published 2 July 2018

Academic Editor: Huseyin Çimenoğlu

Current work was simulated for sliding wear interaction of materials of fuel bundle bearing pad (zircaloy-4) and magazine rotor tube (AISI 304 stainless steel) of Indian Pressurised Heavy Water Reactors (PHWRs). A plan of experiments, based on the techniques of Taguchi, was performed. The objective was to establish a correlation between load and sliding speed with the volume loss and coefficient of friction (COF). These correlations were obtained by multiple linear regressions. The treatment of the experimental results is based on the analysis average and the analysis of variance (ANOVA). Worn surface analyses carried out using SEM and wear mechanisms were identified. ANOVA analysis indicated that load factor has a great influence on the coefficient of friction (~73%). COF suddenly increases to high value after a particular contact pressure due to absence of lubricating film and increase in metal to metal contact. Volume loss of AISI 304 stainless steel and zircaloy-4 is highly affected due to load (~90%) and speed (~65%), respectively. Worn surfaces exhibited deformation, adherence, and compaction of material at all PV conditions. Contact pressures above 475 MPa indicated formation of ratcheting mechanisms and formation of fatigue striation marks. Due to low yield strength of AISI 304 SS, volume loss was on higher side than that of Zr-4.

1. Introduction

Due to their low thermal neutron absorption cross section, good corrosion resistance in water, and good mechanical properties, zirconium and its alloys are preferred materials for nuclear reactor components [1]. Evaluation of tribological properties of zircaloy material is important from viewpoint of its sliding contacts with different materials. Some common applications of zircaloy for Indian Pressurised Heavy Water Reactors (PHWRs) are fuel cladding, coolant tube, and bearing pads for fuel element. Tribological properties of zircaloy material have been evaluated by many researchers; however, considering its application for fuel cladding tube, most of the research work is done for fretting wear analysis [2–5]. Sliding wear studies are rarely performed and only a few cases are available in literature [6, 7]. G. Sharma et al. [6] studied under water sliding wear and friction performance of zircaloy-4 material against 316 stainless steel counterface. Major wear mechanisms identified by them are micropitting, microcutting under low load condition, and delamination of deformed subsurface zones at higher load. P. J. Blau [7] in his work studied dry and oil lubricated performance of few amorphous metals including zircaloy (Zr–Cu–Ni–Ti–Al). He has suggested that more research is needed in order to establish suitability of such materials for specific wear-critical applications. R. Priya et al. [8] studied tribological performance of zirconium-702 and zircaloy-4 in dry and electrolytic environment. They confirmed that synergistic effect of wear and corrosion is more pronounced in Ti and Zr based materials than that in AISI 304L SS.

Tribology research is focusing on statistical analysis of volume loss and friction data in last few decades. R. Sinha

Table 1: Properties of zircaloy-4 and AISI 304 SS [9].

Property	Values	
Material	Zircaloy-4	AISI 304 SS
Composition (wt %)	Sn=1.3, Fe+Cr =0.30, Fe =0.2, Zr =remaining	C= 0.08, Cr=19,, Mn= 2, Ni=9, P= 0.035,S= 0.03,Si=1, Fe=remaining
Density (gm/cc)	6.56	8
Tensile Strength (MPa)	514	505
Yield Strength(MPa)	381	215
Hardness (Rockwell B)	89	70
Hardness (Vickers)	180	129
Elastic Modulus, E (GPa)	99.3	193
Poisson's Ratio, γ	0.37	0.265

et al. [10] performed abrasive wear experiment for Mn/Steel pair using full factorial design on pin-on-disc tribometer. The influence of each input factor was examined to understand its effect for weight loss. The regression equation obtained from analysis of variance table was used for the prediction of weight loss. V. V. Monikandan et al. [11] performed statistical analysis of tribological properties of aluminium matrix composites using full factorial design. ANOVA analysis revealed the statistically and physically significant factors which influence the wear loss and friction coefficient.

One of primary applications of zircaloy-4 in sliding contact is the bearing pads of fuel bundle of Indian PHWRs (Pressurised Heavy Water Reactors). During its lifetime, fuel bundle travels through various locations inside and outside the reactors. To prevent the damage, outer elements of fuel bundle are provided with the bearing pads. During loading to fueling machine, fuel bundle bearing pads come in the sliding interaction with the magazine rotor tube. Considering materials of bearing pad and magazine rotor tube as zircaloy-4 and AISI 304 SS, respectively, similar material pair was taken for experimental evaluation. Operating parameters like sliding speeds and contact pressures were selected considering some extreme operating conditions. The treatment of the experimental results is based on the analysis average and ANOVA.

2. Experimental

2.1. Materials. Sample plates of zircaloy-4 (40 mm × 20 mm × 3 mm dimension) were procured from reputed supplier. Samples were metallographically polished using a polishing machine (Struers Make: LaboPol-5, Denmark) and an average surface roughness (Ra) value of 0.4 μm was achieved. AISI 304 SS balls (12.7 mm dia. AFBMA Grade 25) were selected as a counterface material. Detailed material properties are reported in Table 1.

2.2. Tribological Testing. Tests were performed on wear and friction machine (TE-70, Phoneix Tribology Ltd, UK) with reciprocating ball-on-plate configuration. Tests were carried out in demineralised water (10.5 pH) at room temperature.

Table 2: Assignment of the levels to the factors.

Run	Speed (m/s)	Load (N)
1	0.015	5
2	0.020	8
3	0.025	11

In order to retain uniform test conditions, new ball was used for each test. Specimens were cleaned before the test by immersing in acetone in an ultrasonic bath. Sliding speed (V) and contact pressure (P) were in the range of 0.015, 0.020, 0.025 m/s (7.5, 10, 12.5 Hz frequency) and 475, 555, 616 MPa (5, 8, 11 N load), respectively. Ball was made to slide on the plate sample with selected sliding speeds (keeping sliding amplitude of 0.001 m constant) for different time durations. All tests were performed at constant sliding distance of ~100 m. Each test was repeated three times to verify repeatability of results. Average values of result are reported. Wear track profiles were formed on the plate due to ball sliding. 3D profilometry (Taylor Hobson CCI Optics, UK) was carried out to calculate dimensions of wear scar. Wear mechanisms after sliding were studied in detail by SEM (Carl Zeiss EVO 40, Germany).

2.3. Plan of Experiments (Taguchi's Techniques). For the elaboration of experiments plan, method of Taguchi was used for two factors at three levels. By levels we mean the values taken by the factors. In Table 2 the factors to be studied and the assignment of the corresponding levels are indicated.

The chosen orthogonal array was the L9 (3^2) which has 9 rows corresponding to the number of tests (8 degrees of freedom) with 4 columns at three levels, as shown in Table 3. The factors and the interactions are assigned to the columns. The plan of experiments is made of 9 tests (array rows) in which the first column was assigned to the load (F) and the second column to the velocity (v) and the remaining were assigned to the interactions.

The plan of tests was developed with the aim of relating the influence of the load, velocity in contact with the coefficient of friction, and volume loss. Table 3 presents the results analyzed.

Table 3: Design layout and results for AISI 304 SS and Zr-4.

Run	Load (N)	Speed (m/s)	Coefficient of Friction (μ)	Volume loss (mm^3) For Ball (AISI 304 SS)	Volume loss (mm^3) For Plate (Zr-4)
1	5	0.015	0.234	0.00782	0.00418
2	5	0.020	0.247	0.00947	0.00822
3	5	0.025	0.252	0.00552	0.00671
4	8	0.015	0.244	0.00879	0.00537
5	8	0.020	0.257	0.01058	0.01050
6	8	0.025	0.265	0.01002	0.00785
7	11	0.015	0.272	0.01860	0.00727
8	11	0.020	0.278	0.01760	0.01210
9	11	0.025	0.304	0.01530	0.01010

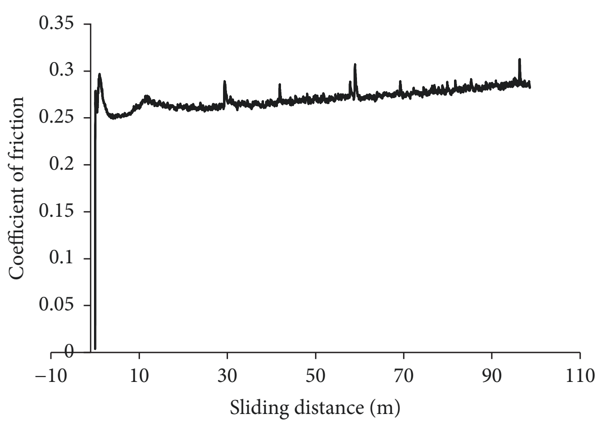

Figure 1: Typical variation of COF with time at 616 MPa contact pressure and 0.015 m/s sliding speed.

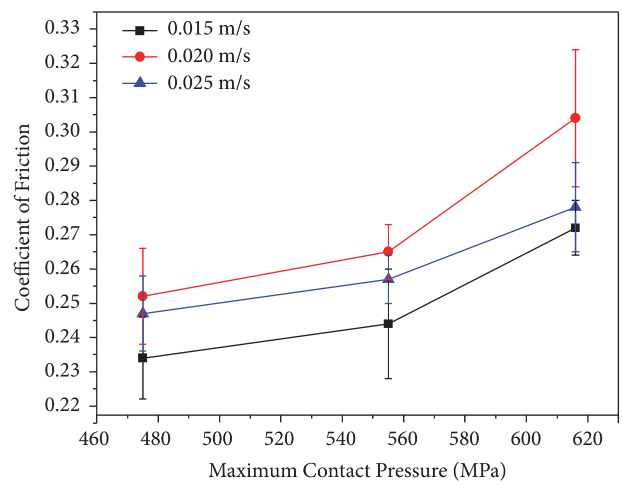

Figure 2: Variation of coefficient of friction with contact pressure and sliding speed.

3. Results and Discussion

3.1. Coefficient of Friction. Figure 1 presents typical variation of coefficient of friction (COF) with sliding distance. Once the graph is stabilized, average value of COF was calculated and reported. Figure 2 presents variation of coefficient of friction with sliding speed and contact pressure. Typical trend is COF increasing with increase in contact pressure. General range of COF is 0.23-0.30.

In general, COF decreases with increase in contact pressure; however other parameters like properties of oxide, generation of wear particles, type of lubrication, etc. may affect the trend. Coefficient of friction is the result of transformation and dissipation of input energy in various forms. Hence coefficient of friction can be presented by the following mathematical formula:

$$\mu = \mu_{adh} + \mu_{def} + \mu_{els\_hys}, \tag{1}$$

where μ_{adh} is due to adhesion of asperities, μ_{def} is due to abrasion or plowing, and μ_{els_hys} is due to elastic hysteresis processes.

Figure 2 is indicating increased rate of COF variation with increase in contact pressure. The reason behind this could be explained by the fact that after a particular high value of contact pressure, rate of oxide layer formation is lower than breakage of oxide layer. This results into interaction of clean metals and hence increased adhesion component of friction.

It is observed from Table 4 that the load factor (P= 72.77%) has great influence on the coefficient of friction. It should also be noticed that the error associated with the table ANOVA for the coefficient of friction was approximately 3.71 %, which is rather low. Regression equation for coefficient of friction is presented by the following formula:

$$\mu = 0.1603 + 0.006722\,\mathrm{F} + 2.367\,\mathrm{v} \tag{2}$$

3.2. Wear Analysis

3.2.1. Zircaloy-4. Figure 3 presents image of wear scar taken by 3D profilometer. Volume of wear was determined from scar measurement. Figure 4 presents variation of volume loss with change in contact pressure and sliding speed of zircaloy-4. It shows decreasing trend with increase in contact pressure.

Table 4: ANOVA for coefficient of friction.

Source	DF	Adj SS	Adj MS	F-Value	P Value	% P
Load, F (N)	2	0.002608	0.001304	39.19	0.002	72.77
Speed, v (m/s)	2	0.000843	0.000421	12.66	0.019	23.52
Error	4	0.000133	0.000033			3.71
Total	8	0.003584				

Table 5: ANOVA for volume loss of Zr-4.

Source	DF	Adj SS	Adj MS	F-Value	P Value	% P
Load, F (N)	2	0.000018	0.000009	79.25	0.001	35.29
Speed, v (m/s)	2	0.000033	0.000016	144.83	0.001	64.71
Error	4	0.0000001	0.0000001			0.2
Total	8	0.000051				

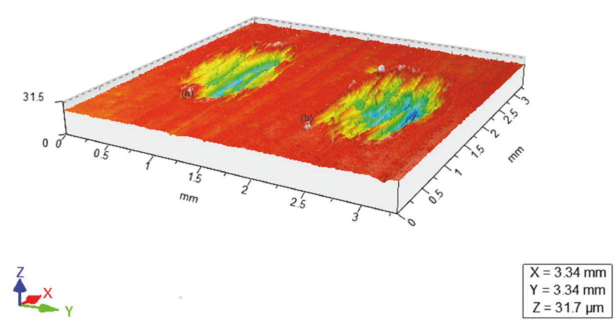

Figure 3: 3D Profilometry at 616 MPa for (a) 0.020 m/s and (b) 0.025 m/s sliding speed.

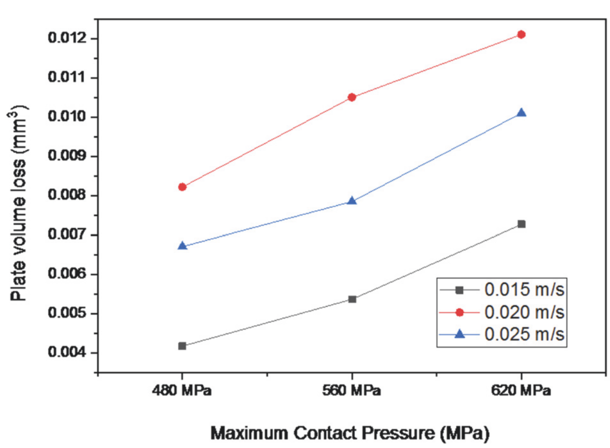

Figure 4: Variation of volume loss of zircaloy-4 plate with contact pressure and sliding speed.

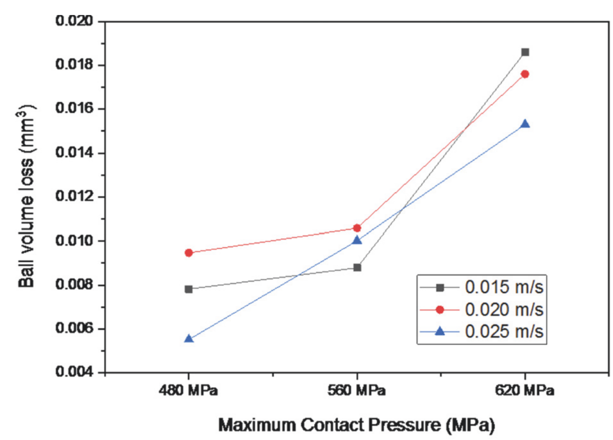

Figure 5: Variation of volume loss of AISI 304 SS with contact pressure and sliding speed.

Due to low viscosity, water is ineffective to act as lubricant; hence material properties play important role for components working in water medium. Formation and fracture of brittle oxides caused metal to metal interaction. Generated wear particle may further dictate the wear behavior of material pair. In current case, due to flow of water, oxide particles might have washed away and hence could not take part further after coming out from metal surface. In general adhesion increases with increase in contact pressure; however properties of wear particles also govern performance. Regression equation for volume loss of Zr-4 is presented by the following formula:

$$(\text{Vol. loss})\ \text{Zr-4} = -0.00180 + 0.000576\,F + 0.261\,v \quad (3)$$

It is observed from Table 5 that the speed factor (P= 64.71%) has great influence on the volume loss. It should be noticed that the error associated with the table ANOVA or the volume loss was 0.2 %.

3.2.2. AISI 304 Stainless Steel. Figure 5 presents variation of volume loss of AISI 304 SS with change in contact pressure and sliding speed. Volume loss is decreasing with increase in sliding speed. Considering ball-on-plate contact geometry (Figure 6), the following formula was used to calculate Hertzian contact pressure or maximum contact pressure along the centre line of circular contact area:

$$p_{\max} = \frac{3F}{2\pi a^2}$$
$$a = \sqrt[3]{\frac{3F\left[\left(1-\nu_1^2\right)/E_1 + \left(1-\nu_2^2\right)/E_2\right]}{4\left(1/R_1 + 1/R_2\right)}}, \quad (4)$$

Table 6: Ratio of contact pressure and yield strength for zircaloy-4 and AISI 304 SS.

Applied Load, F (N)	Contact pressure (MPa)	$\left(\frac{\text{Contact Pressure}}{\text{Yield Strength}}\right)_{Zr-4}$	$\left(\frac{\text{Contact Pressure}}{\text{Yield Strength}}\right)_{AISI\ 304SS}$
5	475	1.24	2.20
8	555	1.45	2.58
11	616	1.61	2.68

Table 7: ANOVA for volume loss for AISI 304 SS.

Source	DF	Adj SS	Adj MS	F-Value	P Value	% P
Load, F (N)	2	0.000151	0.000075	41.04	0.002	90.96
Speed, v (m/s)	2	0.000008	0.000004	2.16	0.231	4.82
Error	4	0.000007				4.22
Total	8	0.000166				

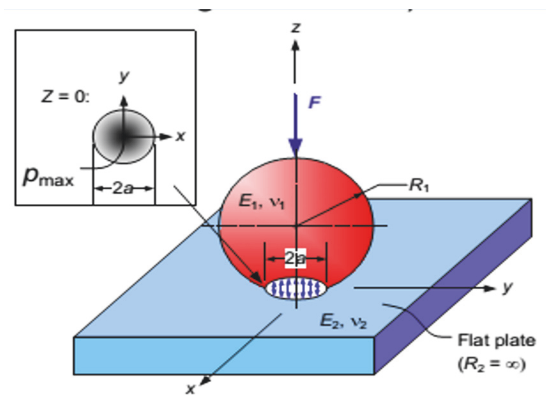

Figure 6: Ball-on-plate contact geometry.

where F is applied load in N, a is radius of circular contact area in mm^2, E_1,γ_1, and E_2,γ_2 are elastic modulus and poisons ratio of ball and plate materials, respectively, and R_1 and R_2 are radius of ball and plate. Ratio of contact pressure and yield strength is calculated and reported in Table 6.

Due to availability of very low contact area for AISI 304 SS ball material, oxide layer, once removed, caused increase in volume loss at certain contact pressure. Properties of wear particle are not much influencing this. Relation between yield strength of material and contact pressure dictates severity of wear. Generally if ratio of contact pressure and yield strength is less than 0.5, mild wear occurs; else severe wear may be observed [12]. Considering above calculation, severe wear may be observed; worn surface analysis was carried out to identify wear mechanisms.

It is observed from Table 7 that the load factors (P= 90.96%) have great influence on the volume loss. It should be noticed that the error associated with the table ANOVA for the volume loss was 4.22%, i.e., rather low. Regression equation for volume loss of AISI 304 SS is presented by the following formula:

$$\begin{aligned}&(\text{Vol. loss})\ \ \text{AISI 304 SS}\\&\quad = 0.0203 - 0.00162\,\text{F} - 0.818\,\text{v} + 0.118\,\text{F} * \text{v}\end{aligned} \tag{5}$$

Analysis of variance (ANOVA) Table 7 includes the F and p values. These are used to determine whether the factors are significantly related to the output (response) or not. Generally, in ANOVA, P value is used to determine whether a factor is significant or not by comparing with an alpha value of 0.05 (used in hypothesis testing). If the p value < 0.05, then the factor is significant. In Table 7, P value is 0.002 which is less than 0.05; thus here input factor load (F) is more significant compared to speed (v) factor. Moreover, percentage of contribution (i.e., % P) is evaluated for both the input factors which showed 90.96 % of contribution for load (F), 4.82 % of contribution for speed (v), and 4.22 % of contribution for error (i.e., for interaction effects and other factors (may be environmental)).

4. Worn Surface Analysis

Generally, sliding under water lubricated environment causes adhesive wear at high spots. At junctions where lubrication is not failed, wear may occur by deformation mechanisms. Similarly individual junction conditions based on type of material in contact can determine whether an oxide layer flakes of or if fracture occurs below the oxide.

Worn surfaces analysis was carried out at various PV conditions. Figures 7(a)–7(i) present the SEM images of worn surfaces. Due to combined effects of repeated cycles and absence of lubricating film, most of the worn surfaces are indicating simultaneous occurrence of several wear mechanisms. Deformation, adherence, and compaction of material were observed at most of the PV conditions. Apart from above, other mechanisms were also observed; some mechanisms are dominating at low and others at high PV conditions.

Microcracks were observed at low PV conditions [Figure 7(a)]. Ratcheting mechanism due to repeated cycles sliding and transferred material was seen at 555 MPa and 0.015 m/s conditions [Figure 7(b)]. With further increase in contact pressure (at same sliding speed), ratcheting mechanisms and striation marks due to fatigue were observed [Figure 7(c)]. Formation of microgrooves due to

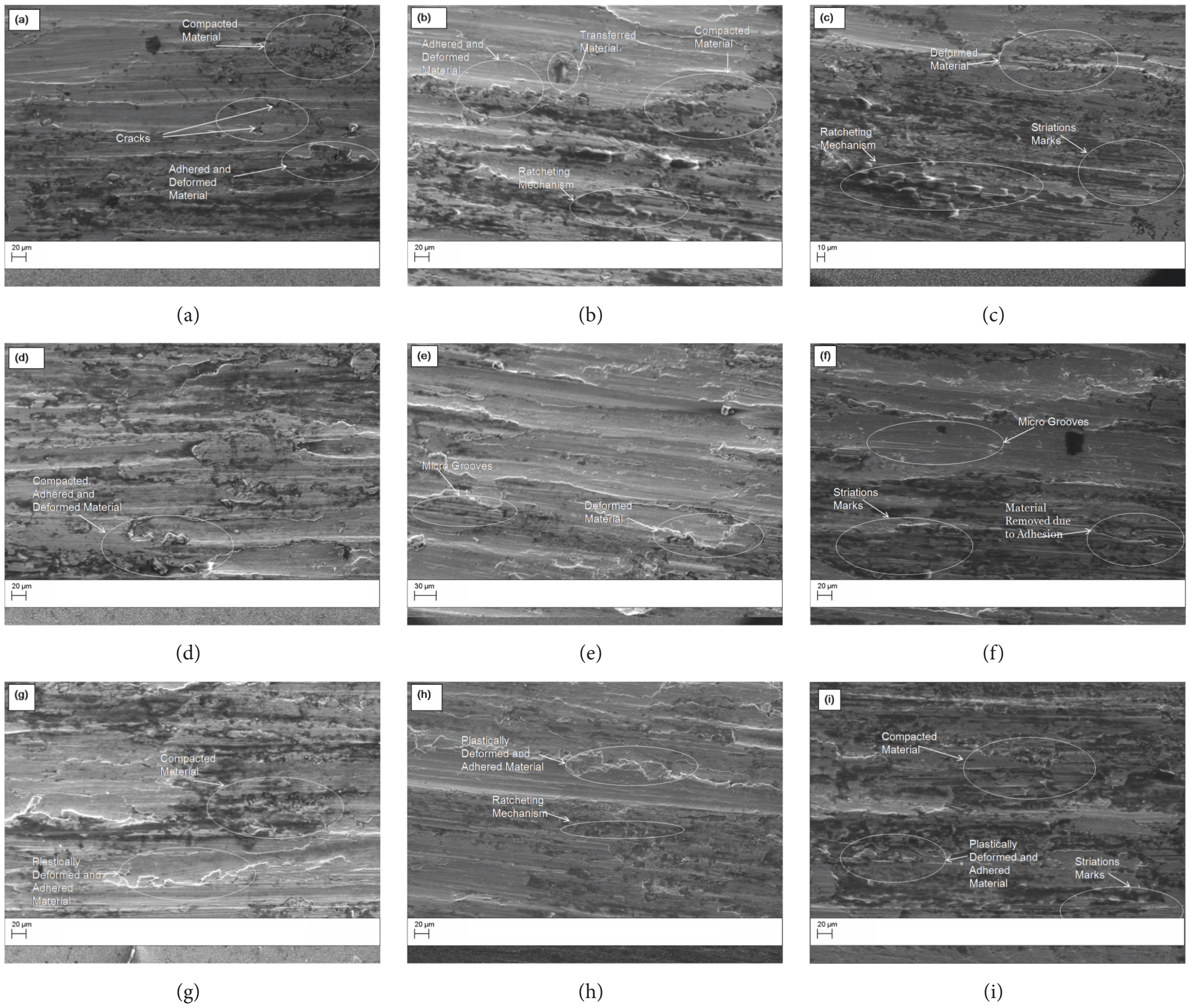

Figure 7: SEM images of worn surfaces of Zircaloy-4 at (a) 0.015 m/s, 475 MPa; (b) 0.015 m/s, 555 MPa; (c) 0.015 m/s, 616 MPa; (d) 0.020 m/s, 475 MPa; (e) 0.020 m/s, 555 MPa; (f) 0.020 m/s, 616 MPa; (g) 0.025 m/s, 475 MPa; (h) 0.025 m/s, 555 MPa; (i) 0.025 m/s, 616 MPa.

absence of lubricating film was observed at 0.02 m/s and 555 MPa/616 MPa contact pressure [Figures 7(e) and 7(f)]. At 0.02 m/s and 616 MPa contact pressure, material pulls out due to absence of lubricating film/ oxide layer observed [Figure 7(f)]. Ratcheting mechanisms and fatigue striations marks were observed at higher PV conditions [Figures 7(h) and 7(i)].

Conclusively, it can be stated that, due to high ratio of contact pressure to yield strength and presence of ineffective water lubricant, deformation, adherence, and compaction of material were observed at all the PV conditions. It can also be added that stress and mechanical properties are primary factors affecting wear mechanisms and both are responsible to increase the severity of mechanisms. High contact pressures above 475 MPa are indicating ratcheting mechanisms and formation of fatigue striation marks. Due to severe plastic deformation, crack generated due to repeated cycle fatigue could not be observed much.

5. Conclusions

Study was carried out for determination of underwater tribological properties of pairing materials of bearing pad (Zr-4) and magazine rotor tube (AISI 304 SS) of Indian Pressurised Heavy Water Reactors (PHWRs). Sliding speeds and contact pressures range were selected considering some extreme operating conditions. Coefficient of friction, volume loss, and wear mechanisms were evaluated. The treatment of the experimental results is based on the analysis average and the analysis of variance (ANOVA). Selected conclusions are as follows:

(i) ANOVA analysis indicated that load factor has a great influence on the coefficient of friction (~72.77%) and volume loss of AISI 304 SS (~90.96%). Speed factor has high influence volume loss of Zr-4 (~64.71%).

(ii) The errors associated with the table ANOVA for the coefficient of friction, volume loss of AISI 304 SS, and volume loss of Zr-4 are only 3.71%, 4.22%, and 0.2%, respectively.

(iii) Decreasing volume loss with increase in contact pressure of Zr-4 was observed. It was explained that generated wear particles might have washed away from interface at the interface and led to decreased volume loss of clean metals. Due to high ratio of contact pressure to yield strength of AISI 304 SS, at any PV value volume loss of AISI 304 SS was higher than that of Zr-4.

(iv) SEM examination indicated deformation, adherence, and compaction of material at all the PV conditions. High contact pressures above 475 MPa indicated formation of microgrooves, ratcheting mechanisms, and formation of fatigue striation marks.

(v) Conclusively, it can be stated that, to keep the wear in mild zone, contact pressure should not exceed 0.5 times the yield strength of material under water environment.

Data Availability

The data used to support the findings of this study are available from the corresponding author upon request.

Conflicts of Interest

The authors declare that they have no conflicts of interest.

References

[1] R. Krishnan and M. K. Asundi, "Zirconium alloys in nuclear technology," *Advances in Tribology*, vol. 4, no. 1, pp. 41–56, 1981.

[2] K. H. Cho, T. H. Kim, and S. S. Kim, "Fretting wear characteristics of Zircaloy-4 tube," *Wear*, vol. 219, no. 1, pp. 3–7, 1998.

[3] O. Vingsbo, A. R. Massih, and S. Nilsson, "Evaluation of fretting damage of zircaloy cladding tubes," *Journal of Tribology*, vol. 118, no. 4, pp. 705–710, 1996.

[4] J. H. Sung, T. H. Kim, and S. S. Kim, "Fretting damage of TiN coated zircaloy-4 tube," *Wear*, vol. 250-251, pp. 658–664, 2001.

[5] H.-K. Kim, S.-J. Kim, K.-H. Yoon, H.-S. Kang, and K.-N. Song, "Fretting wear of laterally supported tube," *Wear*, vol. 250-251, no. 1, pp. 535–543, 2001.

[6] G. Sharma, P. K. Limaye, and D. T. Jadhav, "Sliding wear and friction behaviour of zircaloy-4 in water," *Journal of Nuclear Materials*, vol. 394, no. 2-3, pp. 151–154, 2009.

[7] P. J. Blau, "Friction and wear of a Zr-based amorphous metal alloy under dry and lubricated conditions," *Wear*, vol. 250-251, no. 1, pp. 431–434, 2001.

[8] R. Priya, C. Mallika, and U. K. Mudali, "Wear and tribocorrosion behaviour of 304L SS, Zr-702, Zircaloy-4 and Ti-grade2," *Wear*, vol. 310, no. 1-2, pp. 90–100, 2014.

[9] http://www.matweb.com.

[10] R. Sinha and A. Mukhopadhyay, "Wear characterization and modelling of Mn–steel liners used in rock crushers," *Perspectives in Science*, vol. 8, pp. 374–376, 2016.

[11] V. V. Monikandan, J. C. Jacob, M. A. Joseph, and P. K. Rajendrakumar, "Statistical Analysis of Tribological Properties of Aluminum Matrix Composites Using Full Factorial Design," *Transactions of the Indian Institute of Metals*, vol. 68, no. S1, pp. 53–57, 2015.

[12] R. G. Bayer, *Wear Analysis for Engineers*, HNB Publishing, New York, NY, USA, 2002.